Journal of Undergraduate Chemistry Research, **2026**, 25 (2), 45

USING NAPHTHALENE OVERLAYER TO PROBE THE VOIDED SPACE FORMED DURING ALKANE UNDERLAYER DESORPTION ON Al_2O_3

Vanessa H. Kragelund*, Blake A. Bush*, Mirabelle M. Smith* and A.M. Nishimura†

Department of Chemistry, Westmont College, Santa Barbara, CA 93108

Abstract

Bilayers were formed on Al_2O_3 by physical vapor deposition of aliphatic normal alkanes, followed by the deposition of naphthalene overlayer. Molecular dynamics were monitored in real time by recording the fluorescence spectra of naphthalene as the temperature of the Al_2O_3 was linearly ramped during the temperature programmed desorption (TPD) experiments. Desorption of the alkane underlayer produced a void beneath the suspended naphthalene overlayer. Depending on the alkane used, an additional 7-18 K of thermal energy was required to induce collapse of the overlayer, which occurred concurrently with the maximum in naphthalene excimer intensity. The extent of disorder introduced by this collapse was reflected in both the excimer intensity and the subsequent trap emission that developed during the disorder-to-order transition. As observed for multilayer naphthalene, the trap emission formed over the temperature range of approximately 190-210K with an intensity that was proportional to the degree of disorder present in the reorganizing film.

†Corresponding author: nishimu@westmont.edu *Undergraduate researchers and co-authors

Keywords: adsorption, naphthalene, excimer, vapor deposition, desorption, TPD.

Submitted: June 8, 2026 Accepted: July 2, 2026 Revision received: July 2, 2026 Published: July 3, 2026

Introduction

When molecules are deposited beneath a fluorophoric overlayer, the fluorescence response can serve as a sensitive probe of molecular-scale dynamics. Due to the differences in polarity between the Al_2O_3 surface and the nonpolar alkane adsorbate, clustering and aggregation of the alkane molecules at the surface can be indirectly monitored through changes in the spectral signatures of the fluorophore. As the underlayer subsequently percolates through the fluorophoric adlayer during thermal processing, its interaction with the overlayer can be inferred from changes in both the fluorescence spectrum and emission intensity of the overlayer.[1-6]

Previously, our research focused on the balance between thermally induced motion and dispersion forces acting on the underlayer adsorbate, which was monitored via the fluorescence of the overlayer. Vapor-deposited 1-chloroalkanes on Al_2O_3 were found to aggregate forming adsorption sites when the length of the alkyl moiety was sufficient to accommodate the fluorophore deposited above.[1-6] This observation motivated an ancillary question: by careful selection of the underlayer, can the fluorophore be induced to form specific emissive states—namely trap or excimer emission—as the underlayer percolates through the fluorophoric layer prior to desorption?[1] Any such effects on excimer or trap emission would be expected to manifest as changes in the corresponding fluorescence intensities.

In earlier work, 1,6-dichlorohexane was used as an underlayer and was found to promote trap formation following the disorder-to-order transition in biphenyl.[1,2] In that study, biphenyl served as a probe of changes in surface morphology induced by a homologous series of 1,ω-dichloroalkanes.[7] The effects of the dichloroalkanes were significantly larger than those observed for the corresponding unsubstituted alkanes, a difference that was tentatively attributed to possible π–Cl interactions between the dichloroalkane and biphenyl.[8,9]

The aim of this study was to step back and examine the role of dispersion forces in governing the behavior of small, simple alkane molecules forming the first adsorbed layer on the Al_2O_3 surface. Because the substrate is relatively polar, with exposed oxygen sites, intermolecular dispersion forces between alkane molecules can promote aggregation. For example, Tro et al. reported that in the submonolayer regime, *n*-pentane adsorbed preferentially parallel to the surface due to adsorbate–surface interactions.[10] However, at higher coverages, *n*-pentane adopts a more upright orientation normal to the surface in order to maximize dispersion interactions, leading to enhanced molecular aggregation.[10]

The present study extends this framework by examining the response of a naphthalene overlayer following desorption of the underlying *n*-alkane film. In particular, we consider how the void left by the desorbing underlayer influences molecular dynamics within the fluorophoric film, and whether spectral signatures of naphthalene can be used to determine if the passage of alkane molecules through the overlayer is sufficient to disrupt the stability of the naphthalene excimer and induce an excimer-to-monomer transition during underlayer percolation and desorption. This process is conceptually analogous to sacrificial nanogap formation techniques used in nanofabrication, for example in the creation of controlled cavities in metallic systems such as gold.[11]

Experimental

Naphthalene and alkanes of the highest purity (>99%) were purchased from commercial suppliers (Sigma-Aldrich, St. Louis, MO; TCI, Portland, OR) and used without further purification. Each compound was placed in a sample holder attached to a precision leak valve for vapor deposition. The ultra-high vacuum (UHV) chamber maintained a base pressure of 1×10^{-9} Torr, dominated by residual hydrogen.

A single-crystal Al_2O_3 (0001) substrate (Crystal Systems, Inc., Salem, MA) was mounted on a liquid-nitrogen cryostat via copper posts on either side of the crystal, with a sapphire spacer providing both electrical and partial thermal isolation from the cryostat assembly. Resistive heating of the Al_2O_3 was achieved by passing current through a thin tantalum foil in thermal contact with the substrate.

Substrate temperature was monitored using a type-K (chromel–alumel) thermocouple (Omega, Norwalk, CT) in direct thermal contact with the crystal. Temperature control during temperature-programmed desorption (TPD) experiments was im-

plemented using a LabVIEW-based (National Instruments, Austin, TX) feedback system incorporating a proportional–integral–derivative (PID) controller, enabling a linear heating rate of 1.98 ± 0.01 K s^{-1} (approximately 2 K s^{-1}).

Optical excitation of the fluorophore was achieved using a high-pressure Hg lamp, with the output focused through a 0.25 m monochromator set to λ_0 = 250 nm. Fluorescence emission from the adlayer on Al_2O_3 was collected using a quartz lens and light-pipe assembly coupled through a vacuum feedthrough to the spectrometer.

During temperature-programmed desorption (TPD) experiments, the LabVIEW control program acquired fluorescence spectra every 300 ms in real time using an Ocean Optics SR2 UV–Vis spectrometer (Ocean Optics, Orlando, FL), which is sensitive in the ultraviolet region. Post-acquisition processing of the temperature-dependent spectral array was performed using a MATLAB (MathWorks, Natick, MA) template to generate wavelength-resolved TPD plots presented in the figures.

To ensure a clean substrate, the Al_2O_3 crystal was heated to 300 K after each experimental run. Subsequent temperature ramps to higher temperatures did not reveal the presence of additional adsorbates.[12-16]

The LabVIEW control program received data from a residual gas analyzer (RGA), enabling simultaneous monitoring of both deposition and desorption of naphthalene. Surface coverages (Θ), expressed in monolayers (ML), were determined by calibrating integrated mass spectral signals against an optical interference method. This interference-based calibration provided an accurate deposition rate, with an estimated coverage uncertainty of ±30%, and is described in detail elsewhere.[12-16]

Transmittance of the excitation light was measured using a photomultiplier tube (PMT), the output of which was digitized via a computer-interfaced high-resolution analog-to-digital converter controlled by the same LabVIEW program. A UV short-pass optical filter was placed in front of the PMT to ensure that only the 250 nm excitation light was detected. The PMT voltages corresponding to 0% and 100% transmittance were determined by blocking the excitation beam and by measuring the signal under identical optical conditions with a clean substrate, respectively. In this way, optical transmittance was assumed to vary linearly with PMT voltage. Sources of error included fluctuations in the excitation source intensity and PMT noise, corresponding to low-frequency and high-frequency contributions, respectively. These effects resulted in an overall uncertainty of approximately ±3% in the measured transmittance.

A 10 Hz pulsed quadrupled Nd:YAG laser with output at 266 nm was the excitation source for the laser-induced fluorescence, LIF, measurements. The fluorescence was focused with short focal length lens onto a 0.25 m monochromator equipped with a photomultiplier and λ_0 was set at 398 nm, the peak of the naphthalene excimer fluorescence. The signal from the photomultiplier was amplified and sent to a very fast digitizing oscilloscope, averaged over 4 LIF decay scans and the waveform was exported to the controlling computer that was running the LabVIEW program. The LIF was assumed to decay by first-order kinetics. A least square curve-fitting program was used to determine the slope, i.e. the rate constant, and intercept of this line during the TPD experiment. The intercepts are the initial intensities of the LIF decay. About 2 replicates of TPD runs yielded LIF decay rate constants with a precision of about ± 10%.

Results

Physical vapor deposition of naphthalene produces a physisorbed, amorphous adlayer, as evidenced by the spectral signature of excimer fluorescence.[17] During the TPD experiment, the adsorbate undergoes a transition from this amorphous morphology toward a more ordered state.[12-16]

In bilayer systems, when the underlayer desorbs at a lower temperature than the overlayer, the underlayer molecules must percolate through the fluorophoric film prior to desorption.[1,12-16] Interactions between the percolating molecules and the overlayer can significantly influence the morphology of the fluorophoric adlayer. By judicious selection of the underlayer, the overlayer morphology may be modulated in such a way as to promote or disrupt ordering within the fluorophore layer.

This modulation may occur through several mechanisms. First, the passage of underlayer molecules may promote nucleation sites that facilitate ordering of the overlayer. Alternatively, if the overlayer is already partially ordered, the percolating underlayer may disrupt this structure, increasing the density of defect sites from which radiative relaxation can occur, thereby enhancing monomer emission.[17] A third mechanism is geometric: the presence of the underlayer may increase intermolecular separation within the fluorophore layer, reducing aggregation-induced quenching and thereby increasing the fluorescence quantum yield.[17]

Multilayer naphthalene

Shown in Figure 1 is the wavelength-resolved temperature-programmed desorption (TPD) spectrum of naphthalene. The adlayer formed by vapor deposition of naphthalene on Al_2O_3 is amorphous, as indicated by its characteristic excimer fluorescence. Optical excitation of the singlet electronic state produces broad, featureless emission with a maximum at λ_{max} = 398 nm, consistent with excimer formation.[17]

As the temperature of the Al_2O_3 substrate is increased during TPD, naphthalene undergoes a disorder-to-order transition beginning at approximately 190 K. At this temperature, the emission spectrum evolves from excimer-dominated fluorescence to monomeric emission, characterized by two resolved peaks at 325 and 334 nm. This doublet arises from a vibronic progression associated with C–H bending modes.[17] The emission intensity reaches a maximum at approximately 205 K, followed by complete desorption at approximately 210 K.

n-Pentane/naphthalene

Shown in Figure 2 is the wavelength-resolved temperature-programmed desorption (TPD) spectrum of naphthalene with an *n*-pentane underlayer. For reference, the initial fluorescence intensity immediately following deposition is indicated by a yellow circle. From the intensity–temperature inset, *n*-pentane desorbs at

approximately 132 K (green circle). At this temperature, the excimer emission does not immediately increase to a maximum; instead, the trap emission at 325 nm increases, consistent with transient solvation of the fluorophore as *n*-pentane percolates through the naphthalene overlayer. During this process, the naphthalene molecules become more isolated, and monomeric fluorescence is observed.

As shown in the top-view inset of Figure 2, the emission subsequently reverts to excimer-dominated fluorescence, indicating that the excimer state remains stable and that the disorder-to-order transition is not immediately triggered following complete desorption of *n*-pentane. At approximately 148 K, about 16 K after the *n*-pentane desorption temperature, the excimer intensity increases to a maximum (blue). Beyond this point, thermal quenching leads to a gradual decrease in excimer emission until the onset of the disorder-to-order transition, which occurs at the same temperature as observed for multilayer naphthalene (cf. Figure 1). In contrast, Figure 2 shows that the maximum in trap emission observed at approximately 205 K (red) is significantly enhanced relative to the multilayer reference spectrum (cf. Figure 1).

Figure 3 shows the variation in the enhanced excimer intensity at 148 K (blue sphere in Fig. 2) and the trap emission intensity at 205 K (red sphere in Fig. 2, monitored at 335 nm) as a function of the *n*-pentane coverage relative to naphthalene, expressed as $\Theta_{\text{n-pentane}}$ (ML)/$\Theta_{\text{naphthalene}}$ (ML). All intensities were normalized to their respective initial values (yellow sphere in Fig. 2) to account for small variations in the reproducibility of the nominal 100 ML naphthalene coverage.

The excimer intensity exhibits a monotonic increase with increasing *n*-pentane coverage, followed by a plateau at approximately $\Theta_{\text{n-pentane}}/\Theta_{\text{naphthalene}} \approx 0.41$, corresponding to an approximate molecular ratio of 1:2 (*n*-pentane:naphthalene). This leveling behavior reflects the saturation of the efficiency with which the *n*-pentane underlayer modifies the naphthalene overlayer.

Also shown in Figure 3 is the corresponding trend for the trap emission intensity at 205 K (335 nm). This signal follows a similar dependence on *n*-pentane coverage, with a plateau occurring

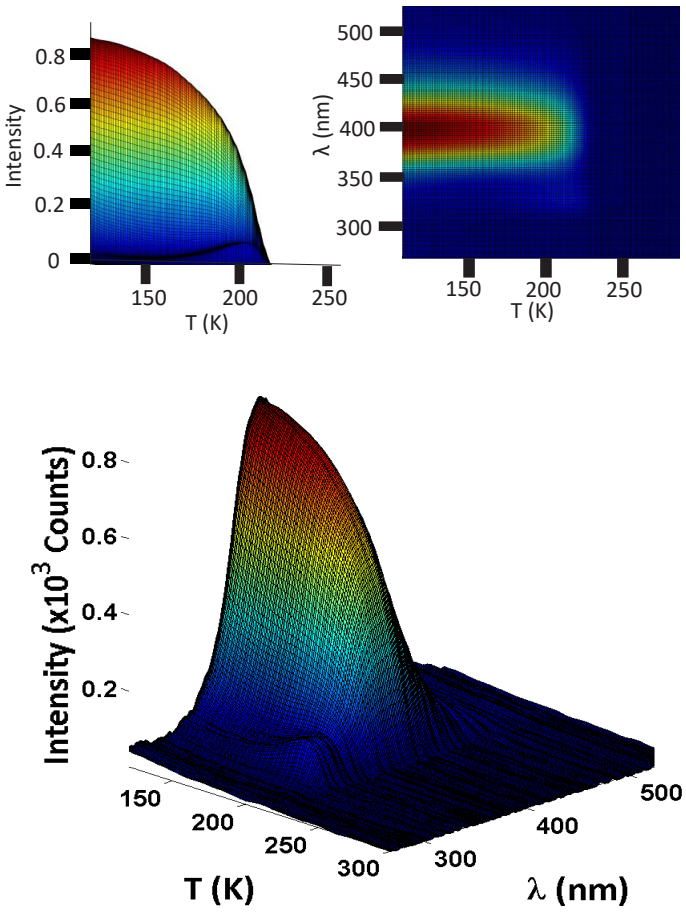

Figure 1. Wavelength-resolved TPD of naphthalene neat with coverage of 87 ML. The excimer has a λ_{max} = 398 nm. The excimer-to-order transition occurs at 205 K during the TPD, but the 325 nm trap emission from the ordered state is barely visible. See left inset: Fluorescence intensity vs. T during the TPD. Right inset: top view.

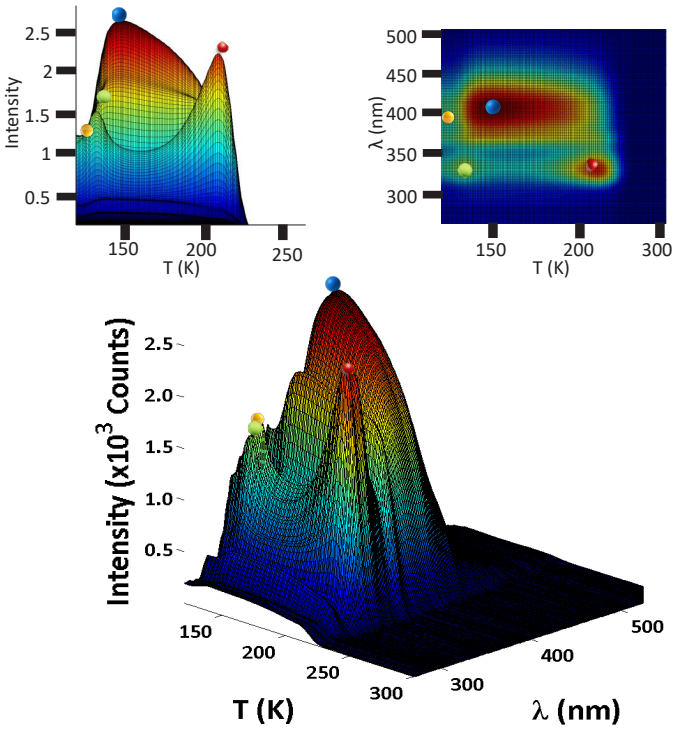

Figure 2. Wavelength-resolved TPD of naphthalene with $\Theta_{\text{naphthalenel}}$ = 100 ML that had been deposited at 117 K with an underlayer of n-pentane with $\Theta_{\text{n-pentane}}$ = 133 ML that was not annealed. Yellow ball points to the initial excimer fluorescence intensity, used to normalize comparative intensities of the excimer or trap. Blue and red balls point to the maximum excimer and trap intensities, respectively. Green ball points to the temperature at which n-pentane desorbed. Left inset: fluorescence intensity vs T during the TPD. Right inset: top view.

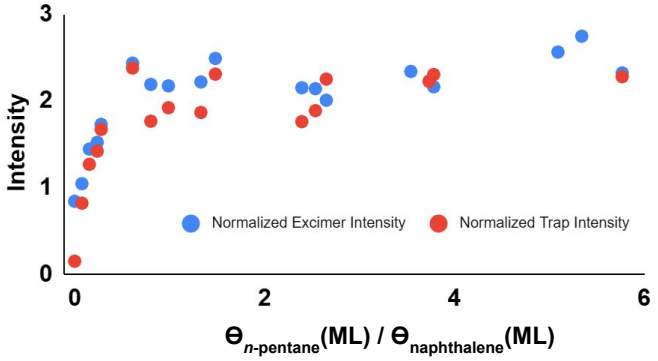

Figure 3. Plot of the normalized fluorescence intensity of the excimer at 398 nm at 148K and the trap at 325 nm at 205 K as a function of $\Theta_{\text{n-pentane}}/\Theta_{\text{naphthalene}}$ with $\Theta_{\text{naphthalenel}}$ = 96 ±11 ML that had been deposited at 117 K with an underlayer of *n*-pentane. To account for the variation in the naphthalene coverages, the intensities were normalized to the initial (t=0) intensities. Changes in slopes for the excimer and trap curves were at 0.41 and 0.30, $\Theta_{\text{n-pentane}}/\Theta_{\text{naphthalene}}$ respectively.

at approximately $\Theta_{n\text{-pentane}}/\Theta_{naphthalene} \approx 0.30$. The comparable trends in both excimer and trap emissions indicate that both processes respond to the degree of underlayer-induced modification of the naphthalene adlayer morphology, with the plateau reflecting a saturation in this effect.

Shown in Figure 4 are the transmittance profiles at several representative *n*-pentane coverages as a function of temperature. Notably, aside from a transient decrease in transmittance attributable to scattering during *n*-pentane percolation through the naphthalene adlayer and subsequent desorption, the transmittance remains relatively constant throughout the temperature-programmed desorption (TPD) experiment. In addition, the baseline transmittance decreases systematically with increasing *n*-pentane coverage, despite a constant naphthalene overlayer coverage.

One possible explanation is that the observed increase in fluorescence intensity is associated with a change in optical absorption arising from structural modification of the fluorophore layer. Specifically, percolation of *n*-pentane through the naphthalene adlayer may induce spatial separation of fluorophoric molecules, thereby reducing aggregation-caused quenching and effectively increasing the fluorescence quantum yield.

This interpretation is supported by lifetime measurements, which show longer excited-state lifetimes in the presence of the underlayer compared to multilayer naphthalene (cf. Fig. S7).

n-Hexane/naphthalene

Shown in Figure 5 is the wavelength-resolved TPD of a bilayer of *n*-hexane and naphthalene. *n*-Hexane desorbed at about 150 K. As was for *n*-pentane, the desorption of *n*-hexane was marked by the increase in the trap intensity (green ball Fig 5) as the *n*-hexane percolated and passed through the naphthalene adlayer. After, the excimer intensity increased until a maximum was observed at 158K (blue ball), which was about 8 K after the desorption of *n*-hexane. In Figure 5, the maximum in the trap fluorescence occurred at 205K, similarly to *n*-pentane as the underlayer.

The plot of the enhanced excimer and trap intensities as a function of *n*-hexane coverage is shown in Figure 6. Here, the leveling of the slope occurred at around 0.86 $\Theta_{n\text{-hexane}}$(ML)/ $\Theta_{naphthalene}$(ML). The plot of the maximum trap fluorescence as a function of coverage appears to level at about 0.40 $\Theta_{n\text{-hexane}}$(ML)/ $\Theta_{naphthalene}$(ML) of *n*-hexane coverage.

n-Heptane/naphthalene

Shown in Figure 7 is the wavelength-resolved TPD of a bilayer of *n*-heptane and naphthalene. *n*-Heptane desorbed at about 157K. The enhanced excimer intensity occurred at 398 nm and at about 175K during the TPD, whereas the peak intensity of the trap occurred at 210 K and at about 335 nm. The *n*-heptane's effect on the excimer was delayed by about 18 K. A plot of both the enhanced excimer intensity and the intensity of the trap are shown in Figure 8. Here, the leveling of the slope occurred at around 0.63

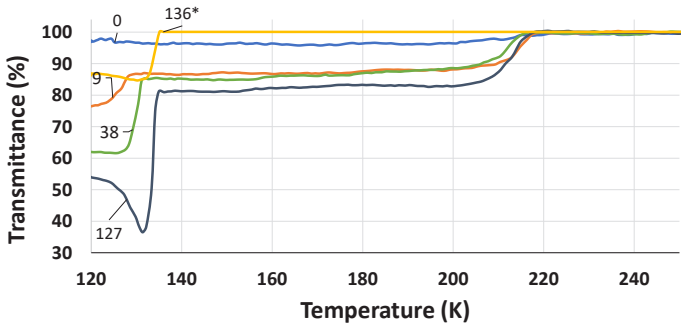

Figure 4. Plot of the transmittance of bilayer with varying n-pentane coverages as a function of $\Theta_{n\text{-pentane}}$ with $\Theta_{naphthalenel}$ = 96 ± 11 ML that had been deposited at 117 K with an underlayer of n-pentane. 0 ⇨ $\Theta_{n\text{-pentane}}$ =0, only overlayer; * ⇨ $\Theta_{naphthalene}$ = 0, only underlayer

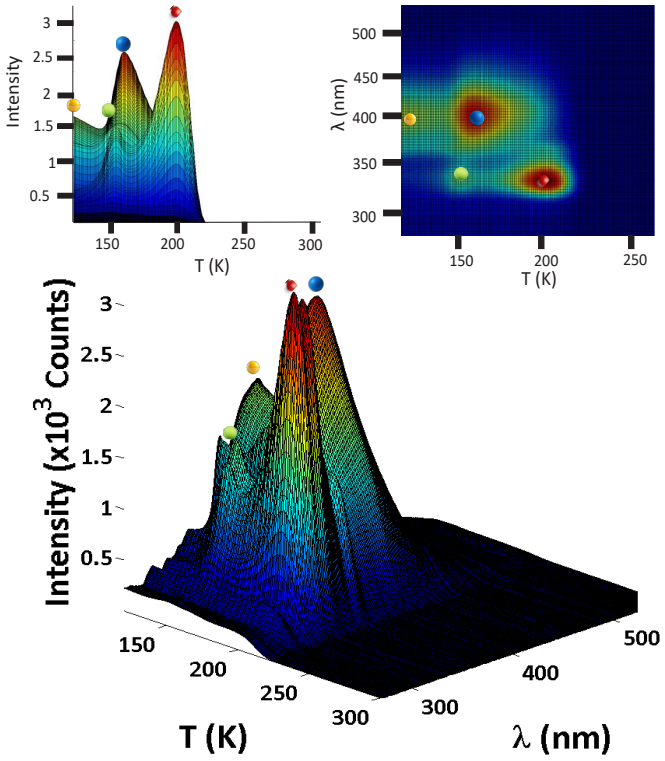

Figure 5. Wavelength-resolved TPD of naphthalene with $\Theta_{naphthalenel}$ = 82 ML with an underlayer of n-hexane with $\Theta_{n\text{-hexane}}$ = 111 ML. Yellow and green balls point to the initial excimer fluorescence intensity and desorption of n-hexane, respectively. Blue and red balls point to the maximum excimer and trap intensities, respectively. Left inset: fluorescence intensity vs T during the TPD. Right inset: top view.

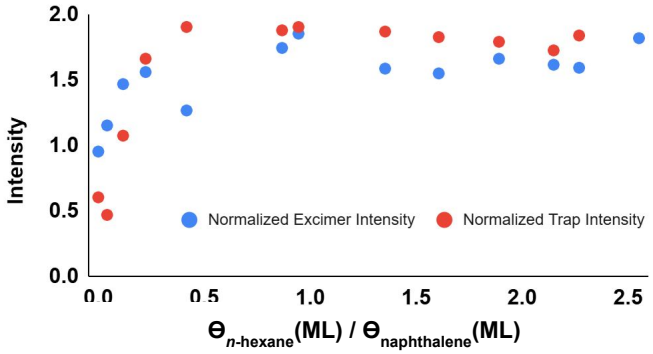

Figure 6. Plot of the normalized fluorescence intensity of the excimer at 398 nm at 158K and the trap at 335 nm at 205 K as a function of $\Theta_{n\text{-hexane}}$ with $\Theta_{naphthalenel}$ = 90 ±29 ML that had been deposited at 117 K with an underlayer of *n*-hexane. To account for the variation in the naphthalene coverages, the intensities were normalized to the initial (t=0) intensities. Changes in slopes for the excimer and trap were at 86 ML and 40 ML, respectively.

$\Theta_{n\text{-heptane}}$(ML)/ $\Theta_{naphthalene}$(ML) ML. The plot of the maximum trap fluorescence as a function of coverage appears to level at about 0.86 $\Theta_{n\text{-heptane}}$(ML)/ $\Theta_{naphthalene}$(ML) of *n*-hexane coverage.

n-Octane/naphthalene

Shown in Figure 9 is the wavelength-resolved TPD of a bilayer of *n*-octane and naphthalene. The desorption temperature for *n*-octane was about 178K. The enhanced excimer intensity occurred at about 190 K, and the peak intensity of the trap was observed at 205 K. The temperature interval between the desorption of *n*-octane and the maximum excimer intensity was about 12 K. A plot of the enhanced excimer intensity and the intensity of the trap is given in Figure 10. Here, the leveling of the slope occurred at around 1.3 $\Theta_{n\text{-octane}}$(ML)/ $\Theta_{naphthalene}$(ML). The plot of the maximum trap fluorescence as a function of coverage appears to level at about 1.6 $\Theta_{n\text{-octane}}$(ML)/ $\Theta_{naphthalene}$(ML) of *n*-octane coverage.

Discussion

To reasonably account for the observed spectral changes in naphthalene with and without an *n*-alkane underlayer during the TPD experiment, we propose that desorption of the alkane creates a voided spatial volume analogous to sacrificial nanogap formation in nanomaterials.[11] In this model, *n*-alkane molecules begin to diffuse through the naphthalene adlayer and transiently solvate individual fluorophoric molecules approximately 10 K prior to their respective desorption temperatures. Evidence for this process is

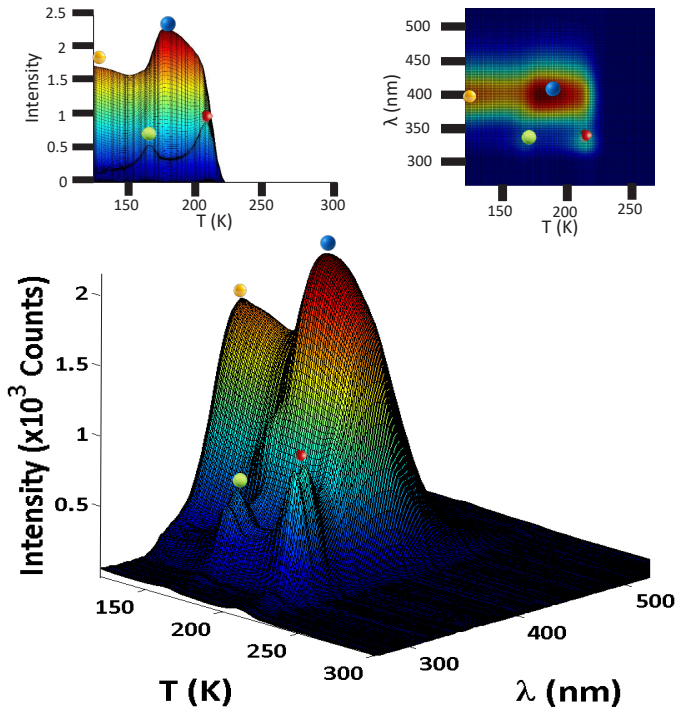

Figure 7 Wavelength-resolved TPD of naphthalene with $\Theta_{naphthalenel}$ = 119 ML with an underlayer of n-heptane with $\Theta_{n\text{-heptane}}$ = 128 ML Yellow and green balls point to the initial excimer fluorescence intensity and the fluorescence from solvated naphthalene molecules, respectively . Blue and red balls point to the maximum excimer and trap ntensities, respectively. Left inset: fluorescence intensity vs T during the TPD. Right inset: top view.

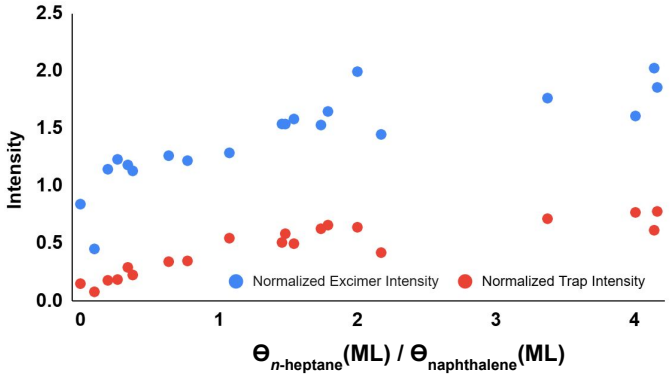

Figure 8. Plot of the normalized fluorescence intensity of the excimer at 398 nm at 190K and the trap at 335 nm at 205 K as a function of $\Theta_{n\text{-heptane}}$ with $\Theta_{naphthalenel}$ = 100 ±22 ML that had been deposited at 117 K with an underlayer of *n*-heptane. To account for the variation in the naphthalene coverages, the intensities were normalized to the initial (t=0) intensities. Changes in slopes for the excimer and trap were at 63 ML and 86 ML, respectively.

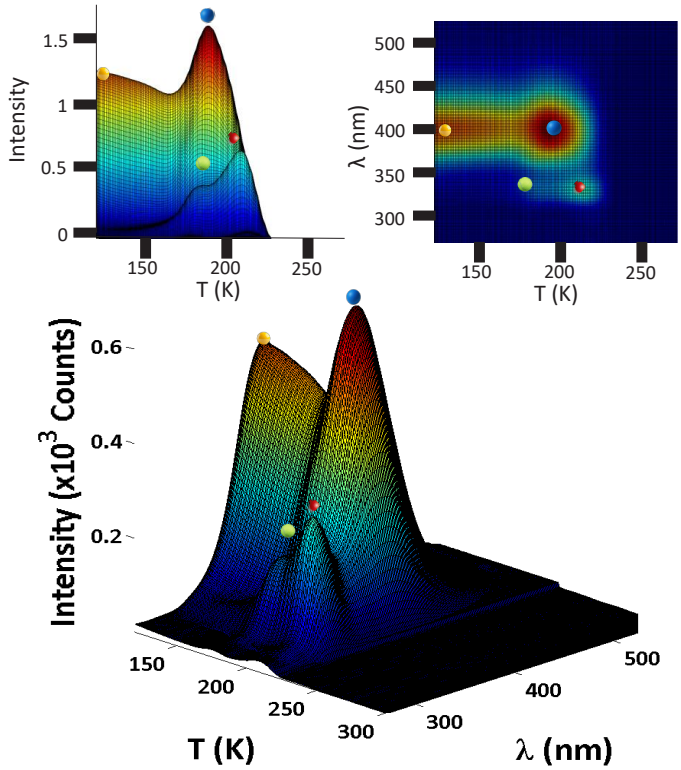

Figure 9. Wavelength-resolved TPD of naphthalene with $\Theta_{naphthalenel}$ = 101 ML with an underlayer of n-octane with $\Theta_{n\text{-octane}}$ = 131 ML.Yellow and green balls point to the initial excimer fluorescence intensity and the fluorescence from solvated naphthalene molecules, respectively . Blue and red balls point to the maximum excimer and trap ntensities, respectively. Left inset: fluorescence intensity vs T during the TPD. Right inset: top view.

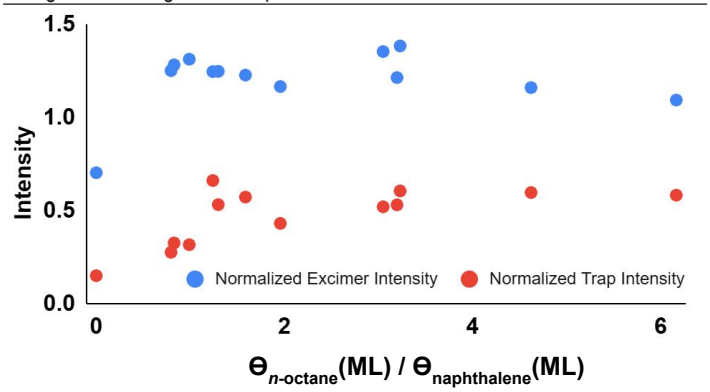

Figure 10. Plot of the normalized fluorescence intensity of the excimer at 398 nm at 158K and the trap at 335 nm at 205 K as a function of $\Theta_{n\text{-octane}}$ with $\Theta_{naphthalenel}$ = 90 ±29 ML that had been deposited at 117 K with an underlayer of *n*-octane To account for the variation in the naphthalene coverages, the intensities were normalized to the initial (t=0) intensities. Changes in slopes for the excimer and trap were at 130 ML and 160 ML, respectively.

provided by the onset of monomer-like emission at low temperature (e.g., Fig. 2, red ball), where increasing intensity is observed from the onset of the TPD at approximately 120 K.

Following alkane desorption, the resulting suspended naphthalene overlayer—a quasi free-standing film—does not immediately collapse. Instead, additional thermal energy is required to overcome the activation barrier for structural reorganization. For an *n*-pentane underlayer, this activation energy corresponds to approximately 16 K above the desorption temperature, while for *n*-hexane, *n*-heptane, and *n*-octane the corresponding values are approximately 8, 18, and 12 K, respectively. The maximum in excimer emission is taken to signify complete collapse of the suspended overlayer, and is interpreted as being dependent on the effective height of the alkane layer normal to the surface.

For *n*-pentane and *n*-hexane, previous studies suggest a predominantly upright orientation on Al_2O_3, driven by dispersion interactions and favorable intermolecular aggregation in the multilayer regime.[10,19] This behavior may be qualitatively analogous to a "canopy" or "dome" of suspended naphthalene overlayer. The trends observed in excimer intensity maxima (Fig. 11) are consistent with this picture.

In contrast, the lower maximum excimer intensities observed for *n*-heptane and *n*-octane may reflect an increased probability of gauche conformations arising from their greater internal conformational freedom.[19,20] This conformational disorder would reduce the effective vertical height of the alkane layer, leading to a lower height of the suspended overlayer. Within this framework, the alkane layer acts as a sacrificial spacer analogous to nanofabricated gap-forming layers.[11]

Consequently, the extent of excimer enhancement may scale with the height of the suspended naphthalene overlayer and thus with the degree of structural order in the alkane underlayer. More conformationally disordered alkanes (e.g., *n*-heptane and *n*-octane) may also introduce a distribution of local collapse events rather than a single coherent collapse, leading to a broadened or temporally distributed relaxation process.

The histogram heights for the four *n*-alkanes can be correlated with their effective molecular dimensions normal to the Al_2O_3 surface. *n*-Pentane and *n*-hexane are assumed to adopt conformations in which all C–C bonds are in the anti configuration, corresponding to an extended geometry oriented approximately normal to the Al_2O_3 plane.

By back-calculating from the decrease in excimer intensity per carbon atom from *n*-hexane to *n*-pentane (Fig. 11), it is estimated that *n*-heptane exhibits approximately one to two fewer carbon atoms contributing to the effective vertical projection. This reduction may be accounted for by the presence of one or two C–C bonds in the gauche conformation. For *n*-octane, a more approximate estimate suggests the presence of two to three gauche conformations, leading to a further reduction in effective height. Within this framework, the effective heights of the *n*-alkanes normal to the Al_2O_3 surface correlate qualitatively with the relative histogram values shown in Figure 11.

At temperatures above the occurrance of maximum excimer intensity, the observed decrease in emission is attributed to thermal quenching.[12-16] The subsequent event in the TPD sequence is the disorder-to-order transition of naphthalene, which is the same transition observed for multilayer naphthalene. This process begins at approximately 190 K and reaches a maximum intensity at around 205 K.

As the disorder-to-order transition proceeds to completion, the maximum intensity of the trap emission is determined by the density of defect sites formed within the emerging ordered layer. This defect density is, in turn, related to the degree of disorder present in the preceding excimer-dominated state (excimer: blue; trap: red in Fig. 11, corresponding color codes for Figs. 2,5,7 and 9). Consequently, the maxima of the excimer and trap emissions are correlated, as shown in Figure 12 and Figures S1–S3, and as discussed in the following section.

This aforementioned correlation also supports the voided space/suspended overlayer model proposed here. To demonstrate this, the trap and excimer intensities for the *n*-pentane underlayer are shown in Figure 12, along with Figures S1–S3 for the other *n*-alkanes. The existence of a correlation between these quantities suggests that greater disorder in the excimer state is associated with higher trap emission intensity, and therefore with an increased density of defect sites in the resulting ordered state.

The slopes of these correlation plots are 1.5 (cf. Fig. 12), 1.4 (cf. Fig. S1), 0.61 (cf. Fig. S2), and 0.62 (cf. Fig. S3) for *n*-pentane, *n*-hexane, *n*-heptane, and *n*-octane, respectively. These differences indicate that the density of defect sites in the ordered crystalline state qualitatively follows the same trend as observed for the excimer response in Figure 11.

The observed trend in the initial excimer intensity (shown in yellow in Figure 11) is also consistent with the trend observed for excimer formation. This behavior can be rationalized in terms of a distance-dependent interaction between the fluorophore and the Al_2O_3 surface. As the separation increases, surface-induced quenching is reduced prior to the onset of TPD. This effect is consistent with the findings of Haynes et al., who reported distance-dependent quenching of phenanthrene excimer fluorescence on Al_2O_3 using Xe spacer layers.[21] Accordingly, the initial excimer intensity reflects the effective height of the naphthalene layer above the Al_2O_3 surface.

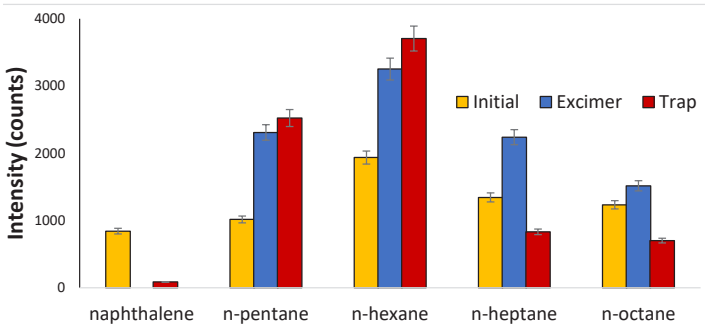

Figure 11. Summary of the average fluorescence intensity initially, maximum excimer intensity and subsequent trap emission intensity after the disorder-to-order transition for the various alkane underlayers. Intensities were averaged past the leveling of the slopes in Figs. 4,6.8 and 10.

The presence of the underlayer leads to increased absorption of excitation light by the naphthalene overlayer, which in turn is expected to enhance both excimer and trap emission intensities (cf. Fig. 4 and S4–S6). The key observation from the transmittance measurements is that absorption of the excitation light is significantly facilitated by the presence of *n*-pentane and *n*-hexane underlayers, whereas this effect is substantially reduced for *n*-heptane and *n*-octane. This trend is consistent with the behavior observed in Figure 11.

As noted in Figures 3, 6, 8, and 10, the number of underlayer molecules required to reach saturation in the excimer and trap emission maxima ("max-out") can be rationalized using a space-filling model of the *n*-alkanes. In this framework, *n*-pentane and *n*-hexane are assumed to adopt predominantly anti conformations, leading to extended structures, whereas *n*-heptane and *n*-octane are more likely to contain one or more gauche conformations on a statistical basis. As a result, the longer-chain alkanes are less effectively extended normal to the surface, folded over and therefore induce a reduced degree of structural perturbation in the naphthalene overlayer during percolation and desorption. This model is consistent with the trends observed in Figure 11.

In conclusion, LIF measurements, excimer fluorescence intensities, the efficiency of underlayer-induced max-out behavior, correlations between trap and excimer emissions, and transmittance data collectively support the voided space/suspended overlayer model proposed here, consistent with the trends shown in Figure 11.

One noteworthy point is that, based on Figure 1, trap emission intensity has previously been interpreted as a weak signature of the disorder-to-order transition, serving as an indicator of the extent to which naphthalene excimer emission converts to an ordered morphology.[1,2,12-16] However, the results reported here—particularly the enhanced intensity of ordered naphthalene fluorescence in the presence of *n*-alkane underlayers—suggest a more refined interpretation. Specifically, for multilayer naphthalene, the disorder-to-order transition appears to yield a highly ordered crystalline morphology with fewer defects than previously assumed. In this view, the trap emission intensity more accurately reflects the formation of a highly ordered state rather than residual disorder. A similar behavior has been observed in biphenyl, where increased structural ordering leads to a significant decrease in fluorescence intensity following the disorder-to-order transition. In the present system, one possible contributing factor is that the naphthalene adlayer may undergo plastic deformation as the substrate temperature approaches the desorption regime, thereby facilitating molecular reorganization into a more ordered structure.

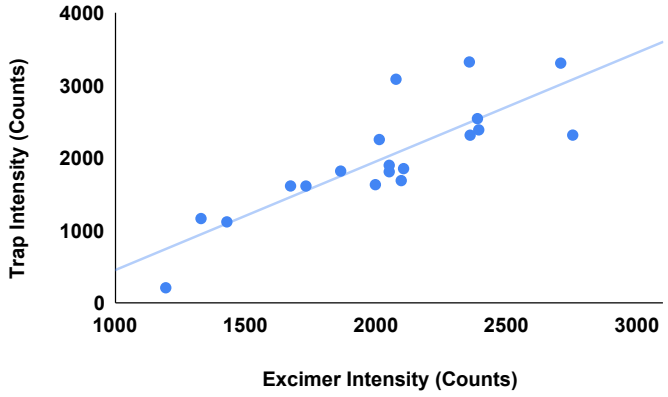

Figure 12. Maximum trap intensity as a function of maximum excimer intensity for various n-pentane/naphthalene coverages. This is an indicator that the two intensities are correlated. $\Theta_{naphthalene}$ = 90 ± 29 ML. Slope = 1.5; R^2 = 0.6

Acknowledgment

The authors would like to thank the John Stauffer Charitable Trust for funding the student stipends for summer research. This work was supported by the donors of ACS Petroleum Research Fund under Undergraduate Research #68385-UR5 .

References

1. J.M. Rosenfeld, R.M. Toepfer, A.O. Lopez, J.C. Nieman, I. Felix, J. Zerwas and A.M. Nishimura, *JUCR*, **2024.** 23, 25-30.
2. I.Z. Song, S.T. Watanabe and A.M. Nishimura, *JUCR*, **2023**, 22, 78-85.
3. M. Frederick, J. Fowkes, *J. Phys. Chem*., **1980**, 84, 510-512.
4. M. Anwar, F. Turci and T. Schilling, *J. Chem. Phys.* **2013**, 139, 214904.
5. T. Arnold, C.C. Dong, R.K. Thomas, M.A. Castro, A. Perdigon, S.M. Clarke and A. Inaba, *Phys. Chem. Chem. Phys*.,**2002**, 4, 3430-3435.
6. T. Arnold, R.K. Thomas, M.A. Castro, S.M. Clarke, L. Messe and A. Inaba, *Phys. Chem. Chem. Phys*., **2002**, 4, 345-351.
7. A.O. Lopez, B.X. Moses, C.D. Tobey, J. Arrieta, M. Ticas, J. Zerwas amd A.M. Nishimura, *JUCR*, 2025, 24, 59-65.
8. K.E. Riley and K.A. Tran, *Crystals*, **2017**,7, https://doi.org/10.3390/cryst7090273.
9. K. Shimizu and J.F. da Silva, *Molecules*, **2018**, 23 2959. https://doi.org/10.3390/molecules23112959
10. C.M. Aubuchon, B.S. Davison, A.M. Nishimura and N.J. Tro, J. Phys Chem. **1994**, 98, 240-244.
11. Z.R. Lawson, A.S. Preston, M.T. Korsa, N. L. Dominique, W.J. Tuff, E. Sutter, J.P. Camden, J. Adam, R.A. Hughes, S. Neretina, ACS Applied Materials & Interfaces. **2022**, 14. https://pubs.acs.org/doi/10.1021/acsami.2c04800.
12. M.K. Condie, Z.E. Moreau and A.M. Nishimura *JUCR*, **2019**, 18, 15-18.
13. M.K. Condie, B.D. Fonda, Z.E. Moreau and A.M. Nishimura, *Thin Solid Films*, **2020**, 697, 137823-137828.
14. B.D. Fonda, Z.I. Shih, J.J. Wong, L.G. Foltz, K.A. Martin and A.M. Nishimura, *JUCR*, **2018**, 17, 32-35.
15. K.L. Nili, Z.E. Moreau and A.M. Nishimura, *JUCR*, **2020**, 19, 19-23.
16. M.K. Condie, C. Kim, Z.E. Moreau, B. Dionisio, K. Nili, J. Francis, C. Tran, S. Nakaoka and A.M. Nishimura, *JUCR*, **2020**, 19, 14-17.
17. J.B. Birks. *Photophysics of Aromatic Molecules*, John Wiley & Sons Ltd., New York, NY (1970), pp. 301-370.
18. Y.N. Imai, Y. Inouye, I. Nakanishi and K. Kitaura, *Protein Sci.* **2008**, 17, 1129-1137.
19. T. Tynkkynen, T. Hassien, M. Tiainen, P. Soininen, R. Laatikainen, *Magnetic Resonance In Chemistry*, **2012**, 50, 598-607.
20. R.M. Slayton, C.M. Aubuchon, T.L. Camis, A.R. Noble and N.J. Tro. *J. Phys. Chem*., **1995**, 99, 2151-2154.

21. D.R. Haynes, K.R. Helwig, N.J. Tro and S.M. George, *J. Chem. Phys.* **1990**, 93, 2836-2847.

Supplemental Material

Correlation of the fluorescence due to the naphthalene trap and excimer intensities: S1-S3

To show that the trap fluorescence intensity is correlated to the excimer intensity, the trap fluorescence intensities were plotted as functions of excimer intensities for various coverages of *n*-alkanes that were shown in Figure 11 for *n*-pentane. S1-S3 are the correlation plots for *n*-hexane, *n*-heptane, *n*-octane, respectively.

Transmittance as a function of n-alkane coverages: S4-S6

These were plotted to show that the decrease in transmittances is related to the coverage of the *n*-alkane while the naphthalene overlayer coverages were held constant at approximate 100 ML. The plot for *n*-pentane was shown in Figure 4. Also shown are transmittances where only naphthalene was deposited and where only the *n*-alkane was deposited. They all show that the higher the *n*-alkane coverage, the more the excitation light is absorbed by the sample. This excludes the possibility that scattering is the major cause, except when the *n*-alkane is desorbing, for the decrease in the overall transmittances during the TPD experiment.

Lifetime (rate constant) measurement of the bilayer by LIF: S7

The results of the LIF measurements of the *n*-alkanes are shown.

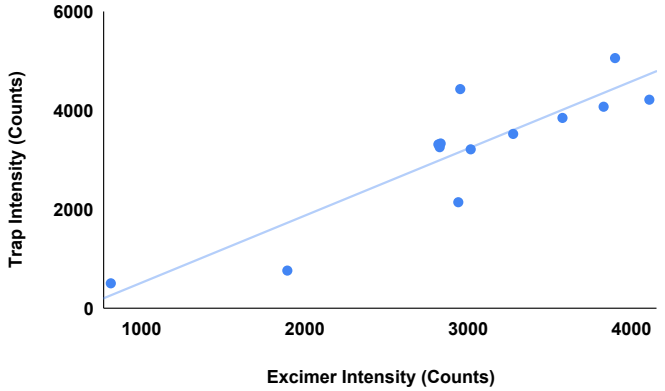

Figure S1. Maximum trap intensity as a function of maximum excimer intensity for various n-hexane/naphthalene coverages. This is an indicator that the two intensities are correlated. $\Theta_{naphthalene}$ = 90 ± 29 ML. Slope = 1.4; R^2 = 0.8.

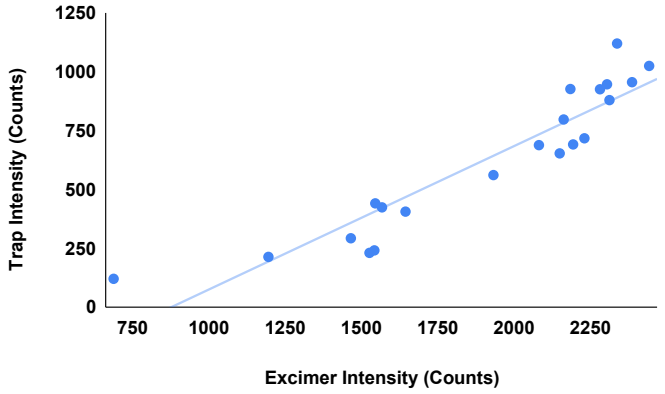

Figure S2. Maximum trap intensity as a function of maximum excimer intensity for various n-heptane/naphthalene coverages. This is an indicator that the two intensities are correlated. $\Theta_{naphthalene}$ = 100 ± 22 ML. Slope = 0.61; R^2 = 0.86

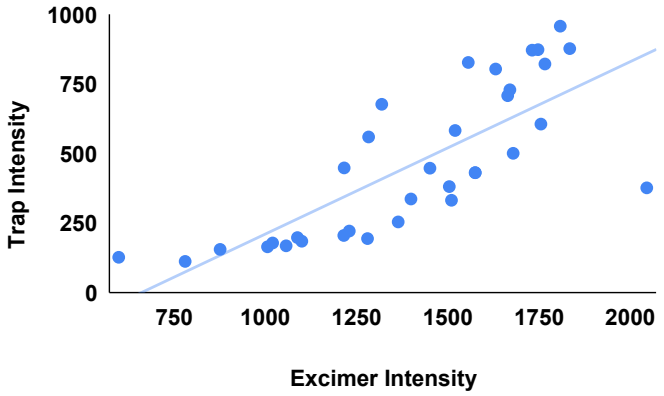

Figure S3. Maximum trap intensity as a function of maximum excimer intensity for various n-octane/naphthalene coverages. This is an indicator that the two intensities are correlated. $\Theta_{naphthalene}$ = 100 ± 22 ML. Slope = 0.62; R^2 = 0.86

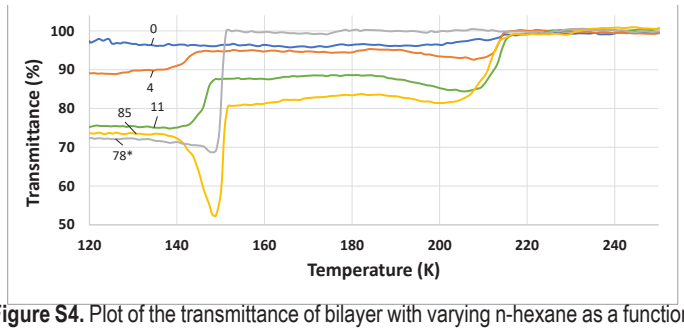

Figure S4. Plot of the transmittance of bilayer with varying n-hexane as a function of $\Theta_{n\text{-hexne}}$ with $\Theta_{naphthalenel}$ = 90 ± 29 ML that had been deposited at 117 K with an underlayer of n-hexane. 0 ⇨ $\Theta_{n\text{-hexane}}$ = 0; * ⇨ $\Theta_{naphthalenel}$ = 0

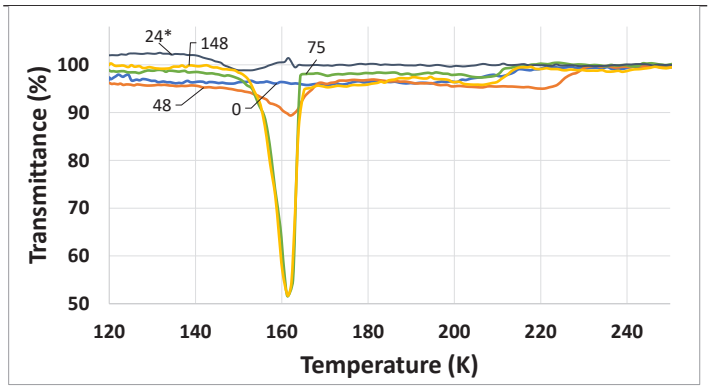

Figure S5. Plot of the transmittance of bilayer with varying n-heptane as a function of $\Theta_{n\text{-heptane}}$ with $\Theta_{naphthalenel}$ = 105 ± 22 ML that had been deposited at 117 K with an underlayer of n-heptane. 0 ⇨ $\Theta_{n\text{-heptane}}$ =0; * ⇨ $\Theta_{naphthalene}$ = 0

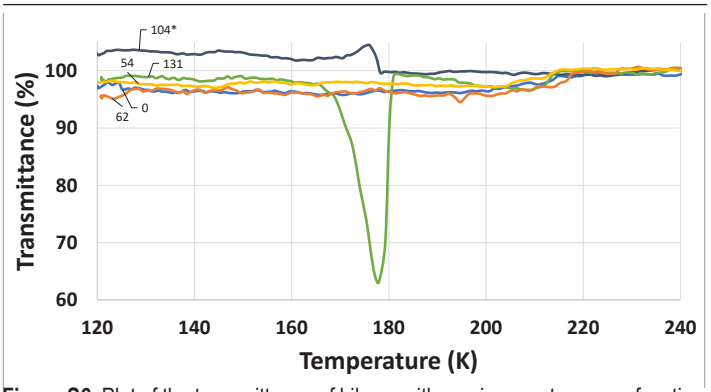

Figure S6. Plot of the transmittance of bilayer with varying n-octane as a function of $\Theta_{n\text{-octane}}$ with $\Theta_{naphthalenel}$ = 97 ± 20 ML that had been deposited at 117 K with an underlayer of n-octane. 0 ⇨ $\Theta_{n\text{-octane}}$ = 0; * ⇨ $\Theta_{naphthalene}$ = 0

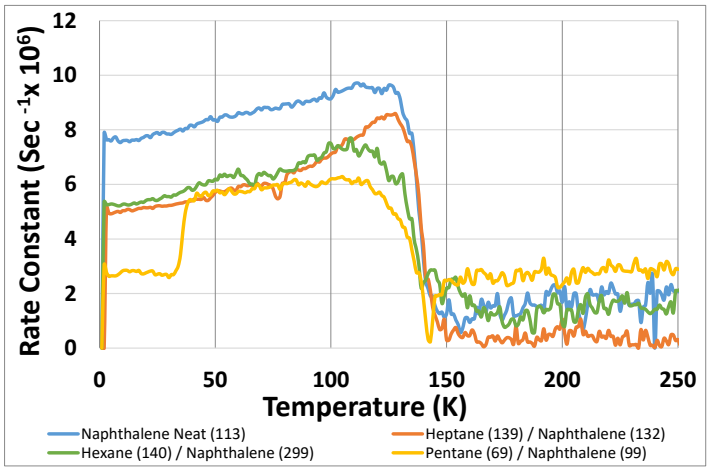

Figure S7. LIF measurements. Rate constants during the TPD. Coverages (ML) in parantheses.